A&A 382, 104–117 (2002)
DOI: 10.1051/0004-6361:20011543

Astronomy & Astrophysics

X–ray and optical monitoring of the peculiar source 4U 1700+24/V934 Her*

N. Masetti[1], D. Dal Fiume[1,**], G. Cusumano[2], L. Amati[1], C. Bartolini[3], S. Del Sordo[2], F. Frontera[1,4], A. Guarnieri[3], M. Orlandini[1], E. Palazzi[1], A. N. Parmar[5], A. Piccioni[3], and A. Santangelo[2]

[1] Istituto Tecnologie e Studio delle Radiazioni Extraterrestri, CNR, via Gobetti 101, 40129 Bologna, Italy
[2] Istituto di Fisica Cosmica ed Applicazioni all'Informatica, CNR, via ugo La Malfa 153, 90146 Palermo, Italy
[3] Dipartimento di Astronomia, Università di Bologna, via Ranzani 1, 40127 Bologna, Italy
[4] Dipartimento di Fisica, Università di Ferrara, via Paradiso 12, 44100 Ferrara, Italy
[5] Astrophysics Division, Space Science Department of ESA, ESTEC, Postbus 299, 2200 AG Noordwijk, The Netherlands

Received 19 September 2001 / Accepted 1 November 2001

Abstract. We report on *ASCA* and *BeppoSAX* X–ray broad band observations of the galactic low-luminosity X–ray source 4U 1700+24 performed on 1995 and 1998, respectively, and on (quasi-)simultaneous ground observations of its optical counterpart, V934 Her, from the Loiano 1.5-meter telescope. In order to better understand the nature of the source we also analyze public archival *ROSAT* and *RXTE* data as well as the *RXTE* ASM light curve of 4U 1700+24; we also re–analyze a 1985 *EXOSAT* pointing. The optical spectra are typical of a M2 III star; this allows us to determine a revised distance to the object of ∼400 pc. While these spectra do not show either any spectral change between the two epochs or any peculiar feature apart from those observed in normal red giants, the spectroscopic measurements carried out in X–rays reveal a complex and long-term variable spectrum, with a clear soft excess. The X–ray spectral properties of the source are best described by a thermal Comptonization spectrum plus a soft energy (<1 keV) excess, which can be modeled in the form of a blackbody emission with $kT_{\rm BB} \sim 1$ keV; the latter component is not detected at the lowest source flux levels. The ratio between the two components varies substantially with the source flux. The X–ray emission from the object appears to become harder as its luminosity increases: indeed, the *RXTE* data acquired during an outburst occurred in October-November 1997 display a hard tail, detected up to 100 keV and modeled with a comptonizing cloud which is hotter and less opaque than that seen in the low intensity state. Apart from erratic shot-noise variability on timescales of tens to thousands of seconds, no significant properties (such as pulsations or QPOs) are found from the timing analysis of the X–ray light curves extracted from the observations presented here. With the new distance determination, the 2–10 keV X–ray luminosity range spanned in the considered observations lies between $\sim 2\times10^{32}$ and $\sim 1\times10^{34}$ erg s^{-1}. All this information, combined with the findings by other authors, allows us to suggest that the scenario which best describes the object consists of a wide binary system in which a neutron star accretes matter from the wind of a M-type giant star. Implications of such a model are discussed.

Key words. X–rays: binaries – stars: individual: 4U 1700+24/V934 Her – stars: neutron – stars: late-type – stars: distances

1. Introduction

In optical astronomy the identification of a binary system derives in most cases from the observation of photometric and/or radial velocity variations at the orbital period; these techniques also allow determining the masses of the two components. This application is of great importance in X–ray binaries, as it helps understanding the nature of the accreting compact object (hereafter labeled also as "primary component", in contrast with the mass donor star which is indicated as "secondary component"). As not all X–ray binaries have optical counterparts known or displaying periodic modulation associated with the orbital period, a further effective criterium in galactic X–ray astronomy for the identification of a binary system harbouring an accreting compact object is often based on the observed X–ray luminosity. For persistent X–ray binaries with a neutron star (NS) or possibly a black hole (BH), luminosities $L_{\rm X}$ of the order of at least 10^{34} – 10^{35} erg s^{-1} are easily reached. The diagnosis of the presence of a NS rather than a BH in bright persistent Low Mass X–Ray Binaries (LMXRBs) is in most cases driven by the

Send offprint requests to: N. Masetti,
e-mail: masetti@tesre.bo.cnr.it

* Partly based on observations collected at the Bologna Astronomical Observatory in Loiano, Italy.
** Deceased.

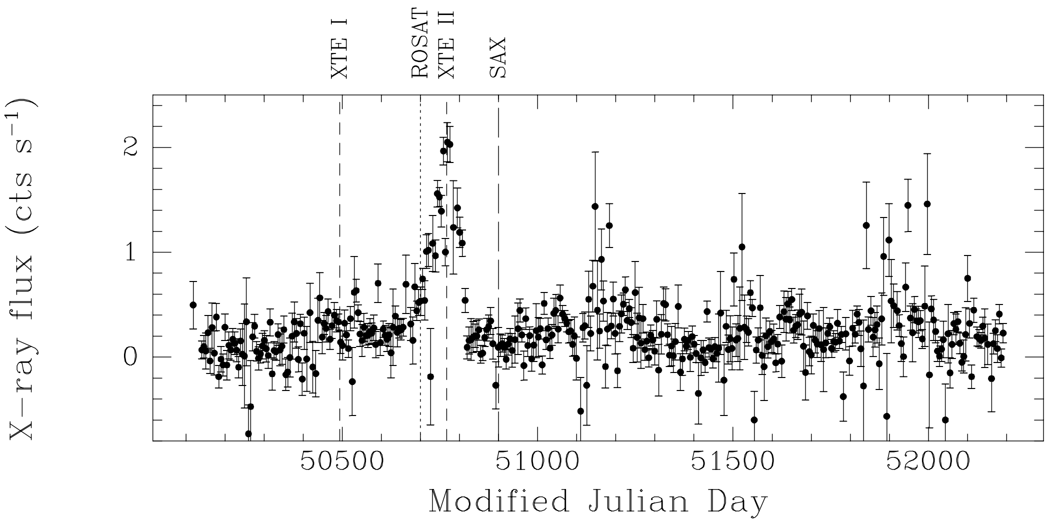

Fig. 1. 2–10 keV 5-day averaged *RXTE* ASM light curve of 4U 1700+24. 1 ASM count s^{-1} roughly corresponds to 13 mCrab assuming a Crab-like spectrum. In the plot the times of the pointed *RXTE*, *ROSAT* and *BeppoSAX* are indicated by the vertical dashed lines (different dashes correspond to different spacecraft). After the bigger outburst occurred around MJD 50750, a series of lower intensity quasiperiodic increases in the X–ray activity from the source are noticed with a recurrence time of about 400 days.

detection of pulsations or thermonuclear X–ray bursts. X–ray binaries harbouring white dwarfs (WDs) also show some distinctive features. As an example, in polars and intermediate polars optical and UV observations often reveal the typical signatures of the presence of a WD in the system. Orbital periods and light curves also add unambiguous and reliable evidence of the presence of WDs in this class of X–ray binaries.

For a number of X–ray sources (see e.g. the catalog of Liu et al. 2001) the identification of a class or even the diagnosis of binarity is rather difficult, especially when the observed X–ray luminosity is $L_{\rm X} \leq 10^{33}$ erg s^{-1}, as they do not easily fit in any of the groups of objects just listed. They do not show any signature in the optical radial velocity to allow the determination of an orbital period, and obviously of the system mass function. Also, they often do not seem to have pulsations or modulations in their X–ray flux which could be related to rotational or orbital periods. They are associated with Population I stars, therefore suggesting a relatively young age, and show persistent emission with a X–ray luminosity varying by at least an order of magnitude. They also display irregular short-term variability, from thousands to tens of seconds and sometimes shorter. The object 4U 1700+24 belongs to this group.

This X–ray source was first detected as a variable object by the satellites *Ariel V* (Cooke et al. 1978) and *Uhuru* (Forman et al. 1978). It shows extremely erratic variations, but no pulsations were ever detected. The rapid (10–1000 s) time variability in X–rays observed with *Einstein* and *EXOSAT* spacecraft is strongly suggestive of turbulent accretion, often observed in X–ray binaries; moreover, the X–ray spectrum of 4U 1700+24 appears rather energetic and was measured up to 10 keV (Garcia et al. 1983; Dal Fiume et al. 1990). The hardness of the spectrum suggests an origin from accretion onto a compact object, but it cannot be used as a decisive parameter.

Its optical counterpart, the bright ($V \sim 7.8$) red star HD154791 (subsequently named V934 Her; Kazarovets et al. 1999), was identified by Garcia et al. (1983) as a late type giant of spectral class M3 II on the basis of the positional coincidence with the error boxes determined by the *Einstein* and *HEAO1* satellites. The optical spectrum of this giant looks quite typical (Garcia et al. 1983; Dal Fiume et al. 1990), with no signs of peculiarities such as emission lines; this fact makes this system unique in the sense that this is the only LMXRB with a "normal" giant star as optical counterpart. However, Gaudenzi & Polcaro (1999) recently found some interesting and variable features in its optical spectrum; these authors gave also a different spectral classification of this star (M3 III). Variable UV line emission was detected by Garcia et al. (1983) and by Dal Fiume et al. (1990) in different IUE pointings, showing at last some unusual features in the emission from this otherwise normal giant. This energetic emission is likely linked to the same mechanism that produces the observed X–ray emission. The X–ray luminosity of the system, computed assuming a distance of 730 pc (Garcia et al. 1983), is $L_{\rm X} \sim 10^{33}$ erg s^{-1}. Infrared emission from this object was observed up to 25 μm with *IRAS* (Schaefer 1986), while no counterpart was detected at radio wavelengths (Wendker 1995).

Recently, during the Fall of 1997, an X–ray outburst peaking at $\approx$30 mCrab in the 2–10 keV band was detected with *RXTE* from 4U 1700+24 (see the long–term X–ray light curve reported in Fig. 1); optical spectra acquired during outburst did not show any change with respect to those obtained during low intensity state (Tomasella et al. 1997). Finally, in spite of various attempts, no evidence of an orbital period was obtained

Table 1. Journal of the X–ray pointings on 4U 1700+24 analyzed in this paper.

Satellite	Obs. start date	Obs. start time (UT)	Exposure (ks)	On-source time (ks)	
EXOSAT	1985 Mar. 15	00:18:24	40.1	36.3	(ME)*
ROSAT	1992 Mar. 22	23:07:33	105.0	7.9	(PSPC B)
	1997 Sep. 8	13:07:32	1164.8	10.6	(HRI)
ASCA	1995 Mar. 8	11:39:26	41.5	22.5	(GIS2)
		11:39:26	41.5	22.5	(GIS3)
		11:39:16	41.5	21.8	(SIS0)
		11:39:16	41.5	21.8	(SIS1)
RXTE	1997 Feb. 14	06:56:32	25.3	11.5	(PCA)
	1997 Nov. 15	11:40:00	12.9	7.9	(PCA)
	1997 Nov. 15	11:40:00	12.9	2.5	(HEXTE)
BeppoSAX	1998 Mar. 27	13:47:22	46.0	12.1	(LECS)
		13:47:22	46.0	24.9	(MECS)
		13:47:22	46.0	12.4	(HPGSPC)
		13:47:22	46.0	11.8	(PDS)

*Results from this observation were already presented by Dal Fiume et al. (1990)

from radial velocity analysis of optical spectra (e.g. Garcia et al. 1983). Therefore, the picture emerging from observations gives only hints in favour of a binary system, as no "classical" features to be associated with the presence of a compact object were ever found.

The aim of this paper is therefore to get a deeper insight on the high-energy properties of this source and to test whether the binary M giant plus accreting compact object scenario for this system is viable. To this task we have monitored this source over a time span of ∼15 years with various X–ray satellites (*EXOSAT*, *ASCA* and *BeppoSAX*). Additionally, in order to achieve a better understanding of the long- and short-term X–ray behaviours of this source, we analyzed still unpublished archival *ROSAT* and *RXTE* public data and we retrieved the data collected with the *RXTE* All-Sky Monitor (ASM). Also, here we report on ground-based optical spectroscopic observations taken at the Loiano 1.5-meter telescope of the Bologna Astronomical Observatory (quasi-)simultaneously with the *ASCA* and *BeppoSAX* pointings.

The paper is organized as follows: Sect. 2 will illustrate the observations and the data analysis, while in Sect. 3 the X–ray and optical results will be reported; in Sect. 4 a discussion will be given, and in Sect. 5 we will draw the conclusions.

2. Observations and data reduction

2.1. *ASCA* and *BeppoSAX* data

In this subsection and in the following one we describe the X–ray observations made with several spacecraft on 4U 1700+24. Table 1 reports the log of all the X–ray observations presented in Sects. 2.1 and 2.2.

4U 1700+24 was observed with the satellite *ASCA* (Tanaka et al. 1994) on 1995 March 8. This spacecraft carried four X–ray telescopes (Serlemitsos et al. 1995) equipped with two Gas Imaging Spectrometers (GIS; Ohashi et al. 1996; Makishima et al. 1996) and two Solid-State Imaging Spectrometers (SIS; Yamashita et al. 1997), each of them sensitive in the 0.5–10 keV range. Standard filtering criteria were applied to the SIS and GIS data: we selected time intervals outside the South Atlantic Geomagnetic Anomaly (SAGA) and for which the elevation angle above the earth limb was $>5°$ and the cutoff rigidity was below 7 GV. Data were extracted from a circular area centered on the source position and with radius $6'$ for the GIS and $3'$ for the SIS. The background was evaluated from blank areas of GIS and SIS images of the 4U 1700+24 field and then subtracted from the source events.

This source was also observed with the Narrow Field Instruments (NFIs) onboard *BeppoSAX* (Boella et al. 1997a) on 1998 March 27. The NFIs include the Low-Energy Concentrator Spectrometer (LECS, 0.1–10 keV; Parmar et al. 1997), two Medium-Energy Concentrator Spectrometers (MECS, 1.5–10 keV; Boella et al. 1997b), a High Pressure Gas Scintillation Proportional Counter (HPGSPC, 4–120 keV; Manzo et al. 1997), and the Phoswich Detection System (PDS, 15–300 keV; Frontera et al. 1997). During all pointings the four NFIs worked nominally and the source was detected by all of them. Good NFI data were selected from intervals outside the SAGA when the elevation angle above the earth limb was $>5°$, when the instrument functioning was nominal and, for LECS events, during spacecraft night time. The SAXDAS 2.0.0 data analysis package (Lammers 1997) was used for the extraction and the processing of LECS, MECS and HPGSPC data. The PDS data reduction was instead performed using XAS version 2.1 (Chiappetti & Dal Fiume 1997). LECS and MECS data were reduced using an extraction radius of 4′ and 3′, respectively, centered at the source position; before extraction, data from the two MECS units were merged together. Background subtraction for the two imaging instruments was performed using standard library files, while the background for the HPGSPC and for the PDS data was evaluated from the fields observed during off-source pointing intervals.

2.2. Other public X–ray data

In order to present a thorough long-term analysis of the X–ray behaviour of 4U 1700+24, we also retrieved from the HEASARC archive[1] all the unpublished X–ray observations on this source. These comprise *ROSAT* and *RXTE* data; we also re-examine an *EXOSAT* pointing already presented in Dal Fiume et al. (1990).

Two pointed observations were performed on 4U 1700+24 with the *ROSAT* satellite (Trümper 1982). The first one was acquired between March 22 and 24, 1992 with the Position Sensitive Proportional Counter (PSPC; Pfeffermann & Briel 1986) unit B, sensitive in the 0.1–2.4 keV range. The second observation was performed with the High Resolution Imager (HRI; Pfeffermann et al. 1987) onboard *ROSAT* between September 8 and 22, 1997, again in the 0.1–2.4 keV range. The HRI detector had a better spatial resolution than PSPC, but it had no spectral resolution, so it could not provide any spectral information on the source. PSPC spectra and light curves were selected by extracting events from a region centered on the source centroid and with 1.′8 radius; good HRI data were instead selected from a circular region with 45″ radius centered on the source. The background was evaluated from blank selected areas in the observed field.

The *RXTE* satellite (Bradt et al. 1993) carries a 5-unit Proportional Counter Array (PCA; Jahoda et al. 1996), which is sensitive in the 2–60 keV energy range and allows a time resolution of 1 μs, and a High Energy X–ray Timing Experiment (HEXTE; Rothschild et al. 1998) composed of two clusters of 4 phoswich scintillation detectors working in the 15–250 keV energy range. This satellite also carries an ASM[2] (Levine et al. 1996) which regularly scans the X–ray sky in the 2–10 keV range with a daily sensitivity of 5 mCrab. Figure 1 reports the complete up-to-date (October 2001) 2–10 keV ASM light curve of 4U 1700+24 starting on January 1996, along with the times of the single *BeppoSAX* pointing, of the second *ROSAT* one and of the two *RXTE* pointed observations. In order to clearly display the long-term trend in the X–ray emission from 4U 1700+24, each point of Fig. 1 is computed as the average of 5 subsequent measurements; given that the single original ASM points we retrieved were basically acquired on a daily basis (i.e. they are one-day averaged measurements), the plot illustrated in Fig. 1 roughly corresponds to a 5-day averaged X–ray light curve.

The *RXTE* pointings were performed on 4U 1700+24 on 1997 February 14 and on 1997 November 15; the latter observation was acquired during the fairly intense X–ray outburst detected by the ASM (see Fig. 1). In the following we will refer to these two *RXTE* pointings as observations I and II, respectively. The PCA instrument detected 4U 1700+24 in both occasions; during the two observations, all five detector units of the PCA were on. Good PCA data were then selected after filtering for low-earth events and high background times. The background was subtracted using the standard PCA background models. Instead, HEXTE detected the source during the second pointing only, when the source was in outburst. In this case, a similar procedure as above was applied to each HEXTE cluster to select good data. Background was determined by periodically rocking the cluster elements on- and off-source. The spectral analysis was performed on good data extracted in the *RXTE* "Standard 2" mode, which provides full spectral information with a time resolution of 16 s.

Finally, the *EXOSAT* observation was acquired on 1985 March 15 with the Medium Energy (ME; Turner et al. 1981) proportional counter (1–50 keV). The source was detected only up to 10 keV during this observation. A more detailed description on this observation and on the applied reduction techniques can be found in Dal Fiume et al. (1990).

Table 2. Journal of the optical spectroscopic observations of V934 Her presented in this paper.

Date	Obs. start time (UT)	Exposure time (s)	Passband (Å)	Slit width (″)
1995 Mar. 8	01:09:03	120	4000–8000	1.5
1998 Mar. 28	03:37:14	300	4000–8000	2.0
1998 Mar. 28	03:43:56	300	4000–8000	2.0

2.3. Optical data

Optical medium-resolution spectra of the star V934 Her were acquired, (quasi-)simultaneously with the *ASCA* and *BeppoSAX* pointings, in Loiano (Italy) with the Bologna Astronomical Observatory 1.52-meter "G.D. Cassini" telescope plus BFOSC on 1995 March 8 and on 1998 March 28. The telescope was equipped with a 1100×1100 pixels Thompson CCD on both occasions. Grism #4 was used on both epochs, providing the nominal spectral coverage indicated in Table 2. The slit width was 1.″5 for the March 1995 observation and 2″ for the March 1998 pointing. The use of this setup secured a final dispersion of 3.7 Å/pix for the spectra acquired during both nights. The complete log of the optical spectroscopic observations presented here is reported in Table 2.

[1] available at: `http://heasarc.gsfc.nasa.gov/cgi-bin/W3Browse/w3browse.pl`

[2] ASM light curves are available at: `http://xte.mit.edu/ASM_lc.html`

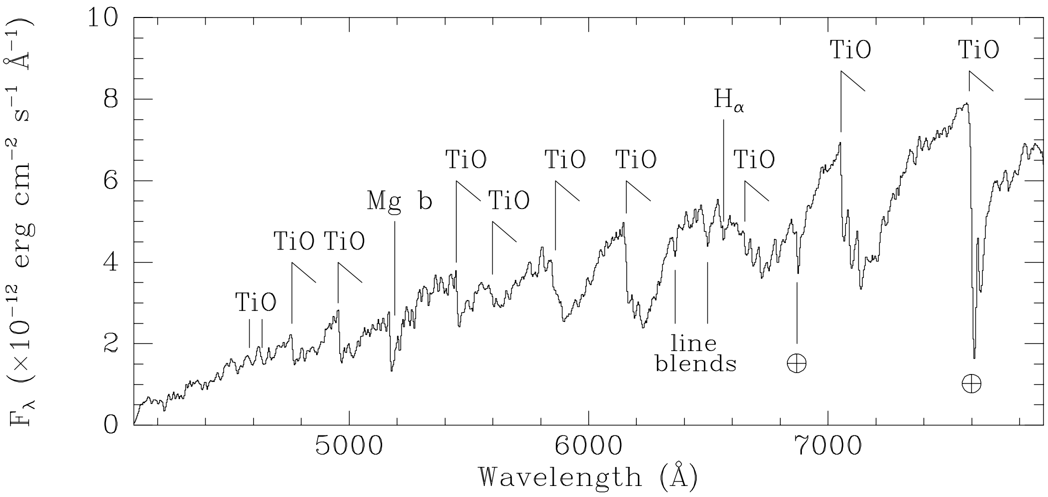

Fig. 2. 4100–7900 Å optical spectum of V934 Her obtained with the Loiano 1.52-meter telescope plus BFOSC on 1998 March 28 and dereddened using $E(B-V) = 0.044$. The spectrum is typical of a star of type M2 III (see text). The telluric absorption bands at 6870 and 7600 Å are marked with the symbol ⊕.

Spectra, after correction for flat-field and bias, were background subtracted and optimally extracted (Horne 1986) using IRAF[3]. Helium-Argon lamps were used for wavelength calibration; spectra taken on March 1998 were then flux-calibrated by using the spectrophotometric standard HD 161817 (Philip & Hayes 1983; Silva & Cornell 1992) and finally averaged together. Correction for slit losses was also introduced. For the March 1995 spectrum no spectroscopic standard was available. The correctness and consistency of March 1998 spectra flux calibration was checked against the optical photoelectric data collected in the $UBVRI$ bands with the 0.6-m Loiano telescope at the epoch in which these spectra were acquired (Diodato 1998). Wavelength calibration was instead checked by using the positions of background night sky lines: the error was 0.5 Å.

3. Results

3.1. Optical spectra and a new distance determination

The flux-calibrated averaged 4100–7900 Å spectrum of V934 Her acquired on 1998 March 28 is reported in Fig. 2. As it appears evident, it is dominated by TiO absorption bands and no emission features are apparent. This is typical of normal M-type giants, as already remarked by other authors (Garcia et al. 1983; Gaudenzi & Polcaro 1999). The H_α line is also detected in absorption. We do not detect the emission wings reported by Gaudenzi & Polcaro (1999) for this line. This might suggest that these wings are variable in intensity due to e.g. changes in the X–ray irradiation (see below), but their non-detection in our spectra might however be also due to our coarser spectral dispersion (3.7 Å/pix, against 1.5 Å/pix of the 6300–7800 Å spectra of Gaudenzi & Polcaro 1999). We also detect, among the main spectral features, the Mg "b" absorption around 5170 Å and two atomic line blends of metal intersystem lines of Fe I, Ti I, Cr I, Ba I, Ca I, Mn I, Co I and Ni I located at 6352 Å and 6497 Å (see e.g. Turnshek et al. 1985). Telluric absorption features are moreover detected at 6870 and 7600 Å.

We next compare the March 1998 averaged spectrum with the one taken on March 1995. As the latter could not be calibrated in flux, we normalized both to their continuum. No appreciable variation in the strength of any absorption line or band between the two epochs is detected in the considered spectral range.

Then, using the Bruzual-Persson-Gunn-Stryker Spectrophotometry Atlas[4] (Gunn & Stryker 1983), we compare the spectrum of V934 Her with that of several red stars whose spectra are present in this atlas. To this task we dereddened our spectrum assuming $E(B-V) = 0.044$; this value is derived from the dust maps by Schlegel et al. (1998). The best match is obtained with the M2 III star HD 104216, whose optical spectrum is strikingly similar to that of V934 Her. A good match, albeit somewhat poorer, is obtained with the star HD 142804 (M1 III). Stars of later or earlier spectral types, as well as (see the classification by Garcia et al. 1983) an M3 II template, the star BD +19°1947 from the Jacoby-Hunter-Christian Spectrophotometric Atlas[5] (Jacoby et al. 1984), provide substantially poorer matches. Thus, we can confidently state that the spectral type of V934 Her is M2 III.

[3] IRAF is the Image Analysis and Reduction Facility made available to the astronomical community by the National Optical Astronomy Observatories, which are operated by AURA, Inc., under contract with the U.S. National Science Foundation. STSDAS is distributed by the Space Telescope Science Institute, which is operated by the Association of Universities for Research in Astronomy (AURA), Inc., under NASA contract NAS 5–26555.

[4] Available at:
`ftp://ftp.stsci.edu/cdbs/cdbs1/grid/bpgs/`.

[5] Available at:
`ftp://ftp.stsci.edu/cdbs/cdbs1/grid/jacobi/`.

This is consistent with the classification made by Gaudenzi & Polcaro (1999), albeit ours appears slightly bluer.

Concerning the more significant difference between our classification and that provided by Garcia et al. (1983), it could be suggested that the star underwent a consistent spectral change somewhere in the past between the years of Garcia et al.'s (1983) and of Gaudenzi & Polcaro's (1999) spectral observations. We however consider this explanation unlikely on the basis of the lack of a strong optical variability and color changes in the $UBVRI$ photometry (Dal Fiume et al. 2000; Diodato 1998), which always shows colors typical of a luminosity class III M-type giant (Lang 1992). Thus, we believe that the spectral classification of V934 Her made by Garcia et al. (1983) using the width of the Ca II K emission line could be biased by the UV variability of this object and by the possible presence of the additional absorption suggested by Gaudenzi & Polcaro (1999). Also, from the data set of Engvold & Rygh (1978), using which Garcia et al. (1983) determined the absolute magnitude M_V in the V band (and then the spectral type) of V934 Her, it seems that the relation between this quantity and the width of the Ca II K line is very steep for giant stars, i.e. a small variation in the line width reflects in a substantial jump of M_V. Therefore we consider the comparison with template optical spectra of stars as a more secure method of spectral classification.

Assuming that V934 Her is a star of spectral type M2 III, we can revise its distance in the following way. Given that the absolute magnitude M_V of a M2 III star is -0.6 (Lang 1992), and that the V magnitude of V934 Her, corrected for interstellar absorption, is $V \sim 7.5$, we obtain, by applying the distance modulus formula, $d = 420 \pm 40$ pc; here the error reflects the uncertainties on the intervening galactic absorption, on the mean V-band magnitude of the star and on the spectral classification. This value is fully consistent with the distance $d = 390 \pm 130$ pc obtained from the annual parallax ($\pi = 2.57 \pm 0.86$ milliarcsec) of this source as measured with the *Hipparcos* satellite (Perryman et al. 1997). In our distance estimate we made the assumption that all of the V-band magnitude comes from the optical companion. This, given the shape of the optical spectrum, is in our opinion reasonable.

Thus, throughout the rest of the paper we will use our revised distance of 420 pc for the 4U 1700+24 X–ray luminosity measurements.

3.2. X–ray data

3.2.1. Positional information

Among all the pointed X–ray observations presented here, the most accurate source position for 4U 1700+24 can be determined using the *ROSAT* HRI data of the September 1997 pointing. The results of the HRI observation on 4U 1700+24 show that the source is located at $\alpha = 17^{\rm h}06^{\rm h}34\overset{\rm s}{.}49$, $\delta = +23°58'18\overset{''}{.}22$ (J2000); the total (boresight plus statistical) error along both coodinates is $8''$.

This position is in total agreement with the one provided in the *ROSAT* PSPC bright source catalogue of Voges et al. (1999). This is true even if only the statistical uncertainty ($0\overset{''}{.}7$) is considered. We also confirm, after comparison with the Digitized Sky Survey, that the only object brighter than the magnitude limit of this survey (i.e. with $R \lesssim 21.5$) lying inside the HRI error circle is indeed the star V934 Her; again, even considering the statistical error only, the HRI localization is fully consistent with the optical counterpart proposed by Garcia et al. (1983), the coordinates of which are given with an extreme degree of accuracy (the reported error is less than $0\overset{''}{.}1$ along both coordinates) in the *Hipparcos* catalogue (Perryman et al. 1997). This further strengthens the association between 4U 1700+24 and V934 Her. This is in agreement, within the uncertainties, with the results independently obtained by Morgan & Garcia (2001) from this same *ROSAT* HRI observation.

3.2.2. Light curves and timing analysis

The long-term (1995/2001) 2–10 keV variability of 4U 1700+24 is evident from the *RXTE* ASM light curve reported in Fig. 1. The increase in the 4U 1700+24 count rate detected in the Fall of 1997 is quite clear, as well as long-term variations of the low state level. However, an apparent recursive behaviour, with peaks which are in any case much less evident than that of Fall 1997, seems to appear in the ASM light curve after the aforementioned outburst. The timing analysis of the 5-day averaged data shows a tentative periodicity of ≈400 days for the outbursting activity of the source. A similar indication is obtained using the dwell-by-dwell and the daily-averaged ASM data sets. Instead, the suggested optical periodicity of 31.41 days reported by Perryman et al. (1997) from *Hipparcos* observations is not found in any of the ASM X–ray data sets.

We also examined the shorter-term X–ray light curves of the pointed observations on 4U 1700+24. These are reported in Fig. 3. All curves are rebinned at 200 s with the exception of those from the two *RXTE* pointings. These are binned with a shorter time interval (16 s) as they allow detecting fast variations with good S/N thanks to the PCA sensitivity.

As one can see, the variability timescale lies between ∼10 s and several thousands of seconds. The substantial erratic variations already detected with *EXOSAT* (Dal Fiume et al. 1990) are clearly present in all observations. The source flux in the *BeppoSAX* pointing is significantly lower than that in the *ASCA* and *RXTE* observations, and comparable with that detected in the *EXOSAT* observation (see next subsection). Likewise, the *ROSAT* light curves at softer (0.1–2 keV) X–ray energies show an erratic variability behaviour similar to that present in the

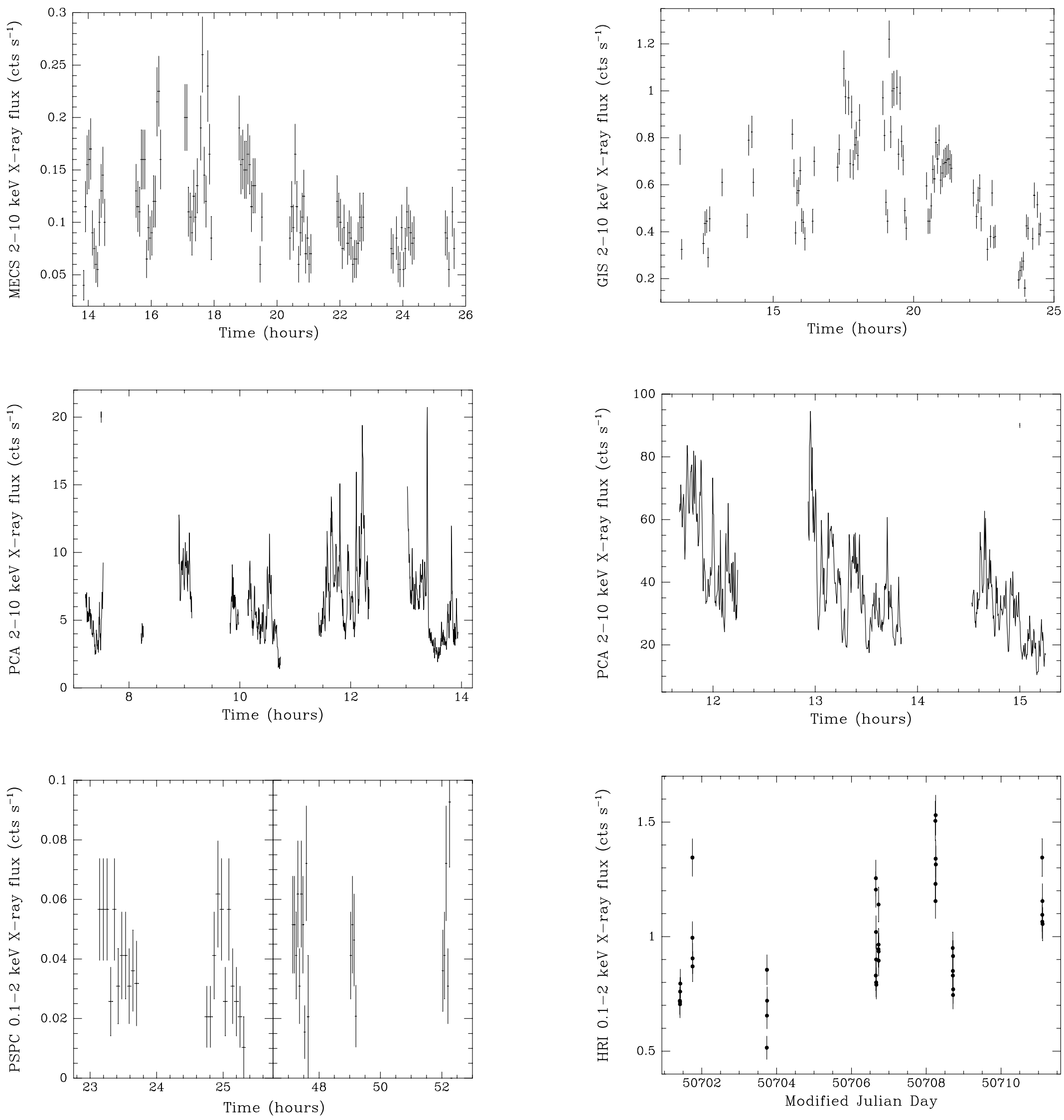

Fig. 3. *(Upper panels)* 2–10 keV background-subtracted light curves of *BeppoSAX* MECS (left) and *ASCA* GIS2+3 (right). Both light curves are binned at 200 s. *(Central panels)* 2–10 keV background-subtracted light curves of *RXTE* PCA observations I (left) and II (right). Both light curves are binned at 16 s. The average uncertainties in the flux measurements of the two pointings are indicated in the upper left and upper right corners of left and right panels, respectively. *(Lower panels)* 0.1–2 keV background-subtracted light curves of *ROSAT* PSPC (left) and HRI (right) pointings. Both light curves are binned at 200 s. Given that, during the PSPC observation, good source events were only recorded in the first ∼2 hours and in the last ∼5 hours of the pointing, we only plot these two time intervals in order to make the light curve of this observation clearer. Fast (10–1000 s) variations are detected during all pointings. 0 hours UT of the day of the beginning of the observation (reported in Table 1) were used as the reference time for panels in which times are expressed in hours.

2–10 keV light curves. Moreover, the longer HRI pointing, performed during the rising branch of the Fall 1997 outburst, shows a hint of increase in the emission with time. These variations do not appear to be correlated with the source hardness, this remaining fairly constant throughout each single pointing.

Timing analysis on the X–ray light curves from the various spacecraft was performed with the FTOOLS[6] (Blackburn 1995) task XRONOS, version 4.02, after having converted the event arrival times to the solar system barycentric frame. The erratic source variability is clearly visible in the Power Spectral Density (PSD); however, no coherent pulsations or periodicities are detected at any significant level in the $f \sim 10^{-4}$–10 Hz frequency range. No indication of the ∼900 s X–ray periodicity found by Morgan & Garcia (2001) from *Einstein* data is found in our data set. Only a $1/f$-type PSD distribution, typical of the shot-noise behaviour evident from the light curves in Fig. 3, is found below 10^{-2} Hz. An example of this is shown in Fig. 4, where a PSD calculated on the time series of the summed 2–10 keV GIS2 and GIS3 count rates binned at 0.1 s is reported. The power density spectra were

[6] Available at:
`http://heasarc.gsfc.nasa.gov/ftools/`.

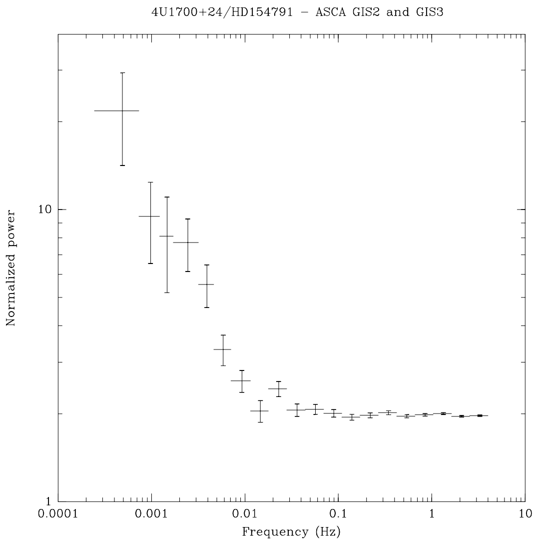

Fig. 4. 2–10 keV PSD of 4U 1700+24 obtained from the summed GIS2 and GIS3 events from the March 1995 *ASCA* observation. The PSD is normalized according to the prescription by Leahy et al. (1983). No coherent oscillation or periodicity is found, while a shot-noise $1/f$-type trend is apparent at low frequencies.

calculated for runs with typical duration of 3000 s. The PSD shown in Fig. 4 is obtained by averaging the temporal spectra of different runs and by summing adjacent frequencies with a logarithmic rebinning.

Likewise, a Fast Fourier Transform (FFT) analysis was made to search for fast periodicities (pulsations or fast QPOs) in the 1–2000 Hz range within the *RXTE* data of observations I and II. In both observations, data in "Good Xenon" mode with a 2^{-20} s (i.e. 1 μs) time resolution and 256 energy bands were available. To search for fast pulsations and/or kiloHertz QPOs we made several FFTs of 16 s long data segments in the 2–10 keV and 10–60 keV energy intervals and with a Nyquist frequency of 4096 Hz. The power density spectra were then averaged for each observation. To reduce the effect of any possible (albeit unlikely) short-term orbital modulation we divided, for each observation, the whole data span in subintervals ~3000 s long (a typical *RXTE* contiguous data segment). We calculated the Z^2 statistics (Buccheri et al. 1983) on each subinterval and finally added together the results. No presence of QPO peaks or of coherent pulsations was detected in both *RXTE* observations.

3.2.3. Spectra

In order to perform spectral analysis, the pulse-height spectra from the detectors of all spacecraft were rebinned to oversample by a factor 3 the full width at half maximum (*FWHM*) of the energy resolution and to have a minimum of 20 counts per bin, such that the χ^2 statistics could reliably be used. For all detectors, data were then selected, when a sufficient number of counts were obtained, in the energy ranges where the instrument responses are well determined. We then used the package XSPEC (Arnaud 1996) v11.0 to fit the resulting broad band energy spectra.

In the broad band *BeppoSAX* fits, normalization factors were applied to LECS, HPGSPC and PDS spectra following the cross-calibration tests between these instruments and the MECS (Fiore et al. 1999). These factors were constrained to be within the allowed ranges during the spectral fitting. Similarly, a constant was introduced between GIS and SIS spectra to allow intercalibration between the two GIS and the two SIS. For the same reason we allowed for a calibration constant between PCA and HEXTE in the *RXTE* data spectral fits. Also, in order to keep into account systematic errors in the response matrices of PCA and HEXTE and the intercalibration uncertainties between these two detectors, a systematic uncertainty of 1% in the count rate was added to their spectra before fitting. Moreover, the spectra from the two HEXTE clusters were fitted independently and the normalization between them was left free given the presence of a small systematic difference between their response. A photoelectric absorption column, modeled using the Wisconsin cross sections as implemented in XSPEC (Morrison & McCammon 1983) and with solar abundances as given by Anders & Grevesse (1989), was applied to all spectral models used in the data analysis and illustrated in this subsection.

BeppoSAX and *RXTE* data show continuum emission above 10 keV coming from the source; during outburst, *RXTE* detects the object up to 100 keV. Moreover, on the low-energy end of the X–ray spectral range, a clear soft excess below 1 keV is apparent from the *BeppoSAX* and *ROSAT* observations (see Fig. 5). In order to find a suitable model which could fit spectra of all observations we started with simple models such as blackbody (BB), disk-blackbody (DBB; Mitsuda et al. 1984), power law, cut-off power law and thermal bremsstrahlung. None of these models could produce an acceptable fit to our X–ray data with the only exception of the *EXOSAT* spectrum which, as already illustrated by Dal Fiume et al. (1990), can be fit either with a power law or with a thermal bremsstrahlung.

Motivated by the suggested similarity in the X–ray temporal and spectral behaviours between γ Cas (Frontera et al. 1987; Haberl 1995) and 4U 1700+24, we next tried to fit the data with the XSPEC models RAYMOND, MEKAL and VMEKAL representing emission from hot diffuse gas (Raymond & Smith 1977; Mewe et al. 1985). This choice was suggested from the work by Kubo et al. (1998) and Owens et al. (1999), who respectively modeled *ASCA* and *BeppoSAX* observations of γ Cas with such a prescription. Our application of these models to our data set is instead far from satisfactory: we get χ^2_ν values between 4 and 8 for all observations even allowing for unplausibly low ($<10^{-11}$) metal abundances with respect to the solar value. Therefore, we reject this representation of the source X–ray spectrum also. Moreover, the partially absorbed bremsstrahlung model used in a preliminary analysis of our *ASCA* and *BeppoSAX* spectra

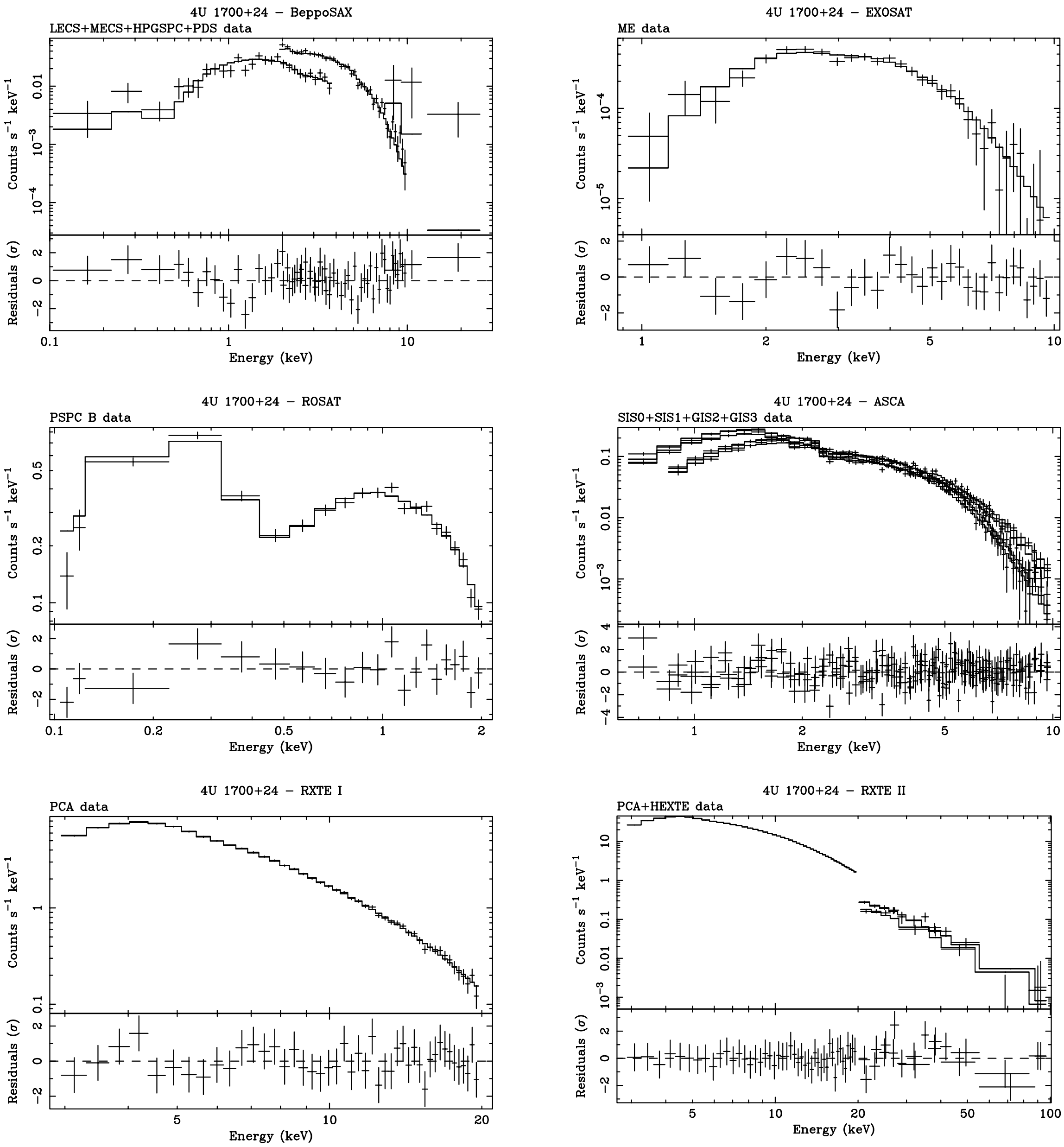

Fig. 5. X–ray spectra of 4U 1700+24 obtained from the spacecraft pointed observations described in the text. The fit residuals using the best-fit models reported in Table 3 are also presented for each observation. In detail, the spectra in the upper row (*BeppoSAX*, 0.1–30 keV, on the left, and *EXOSAT*, 1–10 keV, on the right) are fit with a single, photoelectrically absorbed, Comptonization model; all the other ones in the central (*ROSAT*, 0.1–2 keV, left, and *ASCA*, 0.6–10 keV, right) and lower (*RXTE* I, 3–20 keV, left, and *RXTE* II, 3–100 keV, right) rows are fitted with a photoelectrically absorbed BB+Comptonization model.

(Dal Fiume et al. 2000) gives unacceptable fits when applied to the other observations.

Thus, we tried a composition of two models. The best results are obtained considering a BB plus a Comptonization model. For the latter, we used the first-order modelization by Sunyaev and & Titarchuk (1980; COMPST in XSPEC) for the low-state observations (i.e. all but the *RXTE* II), and the more complete one by Titarchuk (1994; COMPTT in XSPEC) for the outburst pointing. This choice is basically due to two reasons: (i) the lower S/N of the low state spectra does not allow a good constraining of some (or all) parameters of the COMPTT model; (ii) the *RXTE* II observation detects the source up to 100 keV, thus enabling a better sampling of the high-energy component and then a better determination of all COMPTT parameters. It should be noted that the fit to the *RXTE* observation II data is not sensitive to the geometry of the Comptonizing cloud: we therefore decided to assume the (default) spherical geometry.

The BB+Comptonization description of the data allows acceptable fits of all the spectra of our data set. Best-fit parameters are reported in Table 3. The X–ray spectra with the best-fit model superimposed to the data and the fit residuals are shown in Fig. 5. We remark that

Table 3. Best-fit parameters for the X–ray spectra of 4U 1700+24 coming from the observations described in this paper. In all models the hydrogen column density was fixed at the Galactic extinction value $N_{\rm H} = 4\times10^{20}$ cm^{-2}. Luminosities, corrected for interstellar Galactic absorption, are computed assuming a distance d = 420 pc and are expressed in units of 10^{32} erg s^{-1}. In the cases in which the X–ray data could not completely cover the X–ray interval of interest for the luminosity determination, an extrapolation of the best-fit model is applied. Errors and upper limits are at a 90% confidence level for a single parameter of interest. Observations are reported in chronological order from left to right.

Model parameter	*EXOSAT* (1–10 keV)	*ROSAT* (0.1–2 keV)	*ASCA* (0.6–10 keV)	*RXTE* I (3–20 keV)	*RXTE* II (3–100 keV)	*BeppoSAX* (0.1–30 keV)
χ^2/d.o.f.	21.9/29	23.0/16	258/246	26.5/41	71.6/98	68.9/64
BB:						
$kT_{\rm BB}$ (keV)	—	$1.3^{+1.5}_{-0.5}$	$0.86^{+0.07}_{-0.09}$	$1.24^{+0.06}_{-0.04}$	$1.0^{+0.1}_{-0.5}$	—
$R_{\rm BB}$ (m)	—	50^{+90}_{-30}	65^{+14}_{-8}	54^{+14}_{-12}	170^{+100}_{-50}	—
Comptonization:						
kT_0 (keV)	—	—	—	—	$1.4^{+0.4}_{-0.3}$	—
$kT_{\rm e^-}$ (keV)	1.16±0.18	1.8(<8.2)	$2.1^{+0.7}_{-0.4}$	$4.9^{+1.7}_{-0.7}$	$10.8^{+3}_{-1.6}$	$1.16^{+0.05}_{-0.06}$
τ	32^{+30}_{-7}	$9.5^{+4.4}_{-0.6}$	25^{+7}_{-6}	11±2	2.5±0.4	34^{+5}_{-2}
*Normalization**	$2.3^{+0.8}_{-1.1}$	$1.0^{+0.2}_{-0.3}$	$1.41^{+0.14}_{-0.12}$	10±3	$7.4^{+2.5}_{-2.4}$	$1.52^{+0.15}_{-0.16}$
X–ray luminosity:						
0.1–2 keV	—	3.56	—	—	—	1.06
2–5 keV	1.89	—	3.17	8.89	43.9	1.40
5–10 keV	0.83	—	2.27	7.85	57.6	0.68
2–10 keV	2.72	—	5.45	16.7	101	2.07
10–100 keV	—	—	—	—	112	0.047
BB/Comp. flux ratio:						
2–10 keV	<0.05	—	0.70	0.82	0.30	<0.04
0.1–2 keV	—	—	0.27	—	—	<0.03

* In units of 10^{-3}; all normalizations are relative to the COMPST model with the exception of that of the *RXTE* observation II, which is instead referring to the COMPTT model (see text).

the absorption column density $N_{\rm H}$ could not be reliably determined from any of the spectra of our set; therefore, we fixed it to the Galactic value in the direction of 4U 1700+24, which is $N_{\rm H} = 4\times10^{20}$ cm^{-2} (Dickey & Lockman 1990). This value is in agreement with the $N_{\rm H}$ determined from the optical interstellar absorption along that direction (Schlegel et al. 1998) by using the empirical relationship by Predehl & Schmitt (1995).

As it can be seen from Table 3, the *BeppoSAX* and *EXOSAT* spectra (which were taken at the lowest flux levels observed from the source in the present data set) the BB component is not required; for these two spectra, the fit is performed using a COMPST model only, and a 90% confidence level upper limit to the BB flux was computed (see Table 3). In all other cases the BB component is always detected, and the fits performed with this model plus a Comptonization are always much better than those obtained with either single Comptonization or DBB plus Comptonization models.

From our fits there appears to be no need for including an iron emission line around 6.7 keV. In each observation we however computed the 90% confidence level upper limits for the equivalent width (*EW*) of a Fe emission at 6.7 keV assuming different line *FWHM*. The results are reported in Table 4. As one can see, the most stringent limits (coming from *RXTE* II and also, in the narrow-line hypothesis, from *ASCA* observations) imply an *EW* less than 25 eV in the case of a narrow Fe emission and less than 50 eV considering a broad emission line.

Table 4. List of upper limits to the *EW* of the 6.7 keV Fe emission line, assuming different fixed line *FWHM*s, for the various X–ray observations covering that spectral energy. Pointings are listed in chronological order from top to bottom.

Observation	*FWHM*		
	0.1 keV	0.5 keV	1 keV
EXOSAT	<600	<800	<1380
ASCA	<24.4	<53.9	<163
RXTE I	<53.5	<82.0	<208
RXTE II	<24.4	<31.6	<49.7
BeppoSAX	<170	<470	<1290

4. Discussion

4.1. X–ray variability: Accretion onto a NS

The X–ray light curves of 4U 1700+24 illustrated in Figs. 1 and 3, along with the results shown in Table 3 for the various spectral observations presented in this paper, confirm that this source has substantial X–ray variability. In particular, we note that, as the X–ray luminosity $L_{\rm X}$ (say, in the 2–10 keV band) increases, the emission from the object becomes harder: the (5–10 keV)/(2–5 keV) hardness ratio spans from $\sim$0.5 at the lowest flux level sampled here (the *BeppoSAX* observation) to $\sim$1.3 during outburst (the *RXTE* II pointing); likewise, the 10–100 keV flux rises of a factor more than 2000 between these two observations, becoming stronger than the 2–10 keV flux during outburst. The fit parameters, in particular the temperature $kT_{\rm BB}$ and radius $R_{\rm BB}$ of the BB component, as well as the temperature $kT_{\rm e^-}$ and the optical depth τ of the Comptonizing cloud, also show clear correlations (direct for the first three parameters, inverse for the latter one) with $L_{\rm X}$ (see Table 3).

The ratio between the BB and Comptonization components has instead a more complex behaviour: it increases from basically zero to about 0.7 following the X–ray luminosity level in the low-intensity state, and then drops to 0.3 during outburst.

All this is consistent with a model in which enhancement of accreting matter onto a compact object is responsible for the observed spectral shape and variability. Indeed, the two components detected in the X–ray spectrum are suggestive of the presence of a compact object (responsible for the BB emission) which is accreting matter and which is surrounded by a corona of hot electrons; the latter emits hard X–rays by Comptonization of the softer BB photons. In addition, the hardening of the spectrum with increasing luminosity seems to point toward accretion of matter with low specific angular momentum, as suggested by e.g. Smith et al. (2001) and Wu et al. (2002) to explain a similar behaviour observed in other X–ray binaries.

On the contrary, short-period hardness ratio variations are not detected within each single pointed observation. This fast and "colorless" variability is typical of inhomogeneities inside the accretion flow (e.g. van der Klis 1995). This explanation for the fast X–ray variability of 4U 1700+24 is also suggested by the "shot-noise" $1/f$-type PSD associated with all the pointed observations presented here.

Both these longer and shorter term variabilities would point to the presence of variable accretion in this system. The X–ray flux is also much harder and stronger than that expected from coronal emission of a late-type giant star, this being generally 2–3 orders of magnitude lower (Hünsch et al. 1998) than the one detected here even at the lowest luminosity level.

Thus, the X–ray spectral shape and the temperatures of the BB and the Compton cloud would suggest the presence of an extremely compact accreting object, most likely a NS or a BH. Indeed, a WD as accretor is basically ruled out because of the X–ray spectral shape, which (as stated in the previous section) is completely different from that observed by Kubo et al. (1998) and Owens et al. (1999) in the system γ Cas, which is thought to host an accreting WD. Moreover, the high BB temperatures found here are incompatible with those of a WD surface, which basically emits in the UV rather than in the soft X–rays. Also, the X–ray spectrum of 4U 1700+24 observed in outburst is definitely too hard to be emitted by an accreting WD. The BH interpretation for the nature of the accreting compact object also seems less strong than the NS solution because the hard component of the X–ray spectra reported here is generally systematically softer than what expected in the case of an accreting BH (e.g. Barret et al. 2000). So, we suggest that the accreting object is a NS, even if no pulsations or X–ray bursts were ever detected from this source.

It is evident from Table 3 that in every observation the size of the emitting area of the BB is remarkably small, of the order of tens of metres. Shortcomings and limitations of the BB model are known (Gierliński et al. 1999; Merloni et al. 2000); however, these would hardly compensate for the entire difference between the inferred ($\sim$200 m) BB emitting area and that expected in the case of isotropic BB emission from a NS (few km). We therefore suggest that accretion in this system does not take place in a spherical fashion onto the compact object but, rather, that mass coming from the M-type companion in the form of a stellar wind is captured by the NS and then accreted onto a small zone of its surface. An equatorial accretion belt (such as a boundary layer) is disfavoured because the wind has no high intrinsic angular momentum, so a disk can hardly be formed with this accretion mechanism. Indeed, the use of a DBB model instead of a BB produces worse (and in some cases unacceptable) fits to our X–ray data. Also, the non-detection kiloHertz QPOs (which are believed to originate in the inner parts of the disk; see e.g. van der Klis 2000) and of enhanced optical activity (e.g. emission lines) during the Fall (1997) outburst points to the absence of an accretion disk as usually observed in LMXRB where accretion onto the compact object takes place via Roche-lobe overflow of the secondary. Besides, as already remarked by Garcia et al. (1983), in this system the matter transfer onto the compact object is hardly occurring via Roche-lobe overflow as this would produce X–ray emission which is 3–4 orders of magnitude more intense than observed.

An alternative explanation comes by considering a magnetically-driven accretion scenario. In this case, if the magnetic field of the compact object is strong enough, two accretion columns would form and the captured matter flows along field lines and impacts the NS surface in correspondence of the magnetic polar caps. This would however produce pulsations if the rotational and magnetic field axes are not aligned. Given that we do not detect X–ray pulsations from 4U 1700+24, the alignment between these two axes must be invoked to explain the observations. Although this would appear a rather ad hoc hypothesis, we must remark that a similar interpretation has been proposed to explain the absence of pulsations in 4U 1700−37 (White et al. 1983) and, more recently, in 4U 2206+54 (Corbet & Peele 2001), which are believed to host an accreting NS.

Then, if the NS rotation axis is coincident with the magnetic field axis, and the BB emitting area is that of the polar caps only, we could easily obtain, for the emitting area around the NS poles, a size of the order of the BB radius measured from the X–ray spectral fits. Alternatively, we can explain the lack of pulsations from the magnetized accreting NS by assuming a low inclination angle for the system (see next subsection) and the NS rotational axis perpendicular to the orbital plane of the system. In this case, even assuming a non-zero (say, $\approx 20°$) angle between the NS magnetic field and rotational axes, the system geometry is such that we continuously see X–ray radiation from a single polar cap of the NS. Clearly, the emission will not be modulated by the NS rotation in this case also.

We must however note that a further possible explanation for the small BB emitting area size is the following. The estimate coming from our fits is based on the assumption of isotropic emission from the NS surface. It has however been shown (London et al. 1986) that because of cooling and back-warming effects the spectrum at the NS surface, if fitted with a "classic" BB model, can lead to the net effect of overestimating the BB emitting area by as much as 2 orders of magnitude. This would possibly explain our fit results without invoking the funneling of matter onto the NS polar caps by means of an intense magnetic field and the alignment of its axis with the NS rotation axis. In this case, one can overcome the very low ($\sim 10^{-5}$–10^{-6}) accretion efficiency assuming that the NS is orbiting the M giant in a wide orbit (i.e. with separation $a \gtrsim 500\ R_\odot$; see below), and thus only a very small quantity of the emitted stellar wind can be captured and accreted by the compact object.

4.2. A possible scenario for the system

In the hypothesis that the observed X–ray luminosity coming from 4U 1700+24 is due to accretion, an inferred accretion rate onto the NS of $\dot{M} \approx 10^{-14}\ M_\odot\ \mathrm{yr}^{-1}$ is found. This can be explained by assuming a typical mass loss rate via stellar wind of a red giant ($\dot{M} \approx 10^{-9}\ M_\odot\ \mathrm{yr}^{-1}$; e.g. Willson 2000) and an accretion efficiency $\eta = 10^{-4}$ which is quite normal for a NS accreting from the stellar wind (e.g. Frank et al. 1992). The remaining difference between the two above values of $\dot{M}$ can be accounted for by a partial inhibition of the accretion due to the "propeller effect" (Illarionov & Sunyaev 1975), according to which the magnetosphere of the NS acts as a barrier to accretion of matter onto the NS surface. Nevertheless, a small fraction of matter can flow along the magnetic field lines and find a way to the NS. This "leaking" of matter through the magnetosphere has been invoked to explain the X–ray emission of A0535+26 during its low intensity state (Negueruela et al. 2000) and, more recently, of 4U 2206+54 (Corbet & Peele 2001).

The presence of a cold wind from the secondary can be suggested by three further issues: the UV variability, the possible additional absorption detected by Gaudenzi & Polcaro (1999) in the bluest part of their optical spectra, and the fact that the *IRAS* measurements of the mid-infrared source flux at 12 and 25 μm are about a factor three larger than those expected from a normal M giant. Modulations in the wind density, such as density waves produced by pulsations of the M giant envelope, could be responsible for the tentatively observed periodicity in the ASM X–ray light curve. Alternatively, the compact object and the M giant are orbiting around each other along a wide and eccentric orbit, and the X–ray enhancements are due to the transit of the NS through the inner and denser parts of the stellar wind. It is not however clear why no indication of X–ray emission enhancements were present before the large X–ray outburst of Fall (1997). Possibly, this event triggered the mechanism of producing these "periodic" increases of X–ray activity even though at a lower level with respect to the first one.

Whichever the reason for these phenomena, accretion from higher density regions of the stellar wind onto an extremely compact object (very likely a NS) is the most viable explanation for the observed behaviour of luminosity and spectral parameters in the X–ray range. These density variations would modulate the strength of the propeller effect; indeed, the magnetospheric radius is expected to be larger (and thus the magnetospheric barrier should be stronger) when the density of the accreting matter is lower, thus better inhibiting accretion onto the NS. The faster (10–1000 s) variations in the X–ray luminosity are instead most probably produced by small-scale inhomogeneities of the accretion flow onto the compact object.

Concerning the "normal" spectrum of the optical counterpart, V934 Her, we note that the bolometric luminosity (most of which is emitted in the optical and near-infrared bands) of a M2 III giant is 550 $L_\odot$ (Lang 1992), which is a factor $\sim$200 higher than the L_X measured during outburst from 4U 1700+24 (see Table 3). This would explain the absence in the optical spectrum of emission features (Tomasella et al. 1997) which could be induced by the possible X–ray irradiation during outburst. For instance, the object GX 1+4, which is often compared to 4U 1700+24 as it is the only other LMXRB with a M giant secondary, displays a composite optical spectrum with numerous emission lines (Chakrabarty & Roche 1997); it however has a bolometric flux from the secondary which is 4 times less than the X–ray luminosity of the compact object (a pulsating NS). This can naturally explain the difference between the optical spectra of these two X–ray binaries. Possibly, the emission wings from Balmer and He lines detected by Gaudenzi & Polcaro (1999) in V934 Her could be an indication of emission coming from small regions of the accretion flow or of the M giant surface heated by the X–ray irradiation.

Next, we would like to briefly discuss about the possible size and orbital period of this system. In order to match the very low (<3 km s^{-1}) projected orbital velocity of the secondary star obtained from optical spectroscopic measurements (Garcia et al. 1983) with the fact that the accretion most likely occurs via stellar wind capture, the system should be fairly wide. Indeed, considering $P_\mathrm{orb} \approx$ 400 days and assuming typical masses for a NS (1.4 $M_\odot$) and a M2 III star (1.3 $M_\odot$; Lang 1992), we get by applying Kepler's third law an orbital separation $a \approx 300\ R_\odot$, thus substantially larger than the radius of a M2 III giant (≈60–70 $R_\odot$; Dumm & Schild 1998). In this case the orbital velocity would however be ∼10 times larger than the upper limit to its projected value measured by Garcia et al. (1983). Thus, the above prescription would be valid only if the system has a low inclination angle ($i < 10°$). Alternatively, considering higher vales for i and keeping the orbital separation larger than the radius of a M2 III star, we obtain longer (2–5 years) orbital periods. In the latter case, the tentative 400-day X–ray activity periodicity of the source would be tied to density waves in the stellar wind and thus to possible secondary star pulsations, rather than to the orbital modulation.

Finally, we want to draw the attention of the reader on the fact that this low-luminosity source can be studied in the high energy range because of its proximity. Indeed, if it were at, say, 4 kpc from earth, its emission would have been hardly detected by any of the spacecraft quoted above. Therefore, several other systems similar to 4U1700+24/V934 Her might be present throughout the Galaxy, and its "uniqueness" is actually a selection effect due to a combination of its low X–ray emission and its closeness.

5. Conclusions

We analyzed the existing and mostly still unpublished data set of X–ray pointed observations on the source 4U 1700+24. These observations span a time baseline of more than 15 years and were acquired with 5 different spacecraft. In parallel, we presented (quasi-)simultaneous ground-based optical spectroscopic observations.

The optical data allow us to show that the optical counterpart is a red giant of spectral type M2 III with no significant peculiarities. With this more accurate classification we can determine a better distance estimate to the object, which lies at ∼400 pc from earth. The X–ray data show strong and fast erratic shot-noise variability with no hardness variations connected with the intensity changes. On the longer term, instead, the X–ray emission from the source becomes harder as the luminosity increases. No pulsations, periodicities or quasi-periodic oscillations (QPOs) are detected in the X–ray light curve with the possible exception of a tentative long-term periodicity of ≈400 days. X–ray spectra can generally be well described using a BB+Comptonization model, although the BB component is practically undetected at the lowest X–ray intensity states. This spectral modelization is suggestive of a compact object harboured in this system and accreting matter from the giant M star positionally coincident with the X–ray localization. The rather high BB and Comptonizing cloud temperatures along with the X–ray spectral shape of the Comptonization component suggest the presence of a NS as the accreting collapsed object.

The observed 2–10 keV X–ray luminosity of the source ranges from $\sim 2\times10^{32}$ erg s^{-1} during the low intensity state to 10^{34} erg s^{-1} at the peak of the outburst which occurred in the Fall of 1997. These values point to accretion from a stellar wind rather than via Roche-lobe overflow, in which case one would expect X–ray luminosities larger by 3–4 orders of magnitude. The fast X–ray variations are in this hypothesis connected with inhomogeneities in the accreted wind.

The markedly small size of the BB emitting area inferred from our fits to the X–ray data could indicate that wind accretion is funneled by the NS magnetic field onto the magnetic polar caps; given that no X–ray pulsations are detected from the object, it would be possible that the magnetic and rotational axes of the NS are coincident, or that the system has a very low inclination. In addition, the magnetic propeller effect would explain the very low accretion efficiency. Alternatively, cooling effects on the NS surface could explain this small BB emitting area, without invoking a substantially strong magnetic field for the collapsed object; in this case, the low accretion efficiency may be interpreted by assuming a wide binary separation for the system. Indeed, given the known upper limit to any orbital motion of the M giant, only systems with wide (hundreds of $R_\odot$) separations could be fit into the outcoming observational picture.

Acknowledgements. This work is supported by the Agenzia Spaziale Italiana (ASI) and the Italian Consiglio Nazionale delle Ricerche (CNR). *BeppoSAX* is a joint program of ASI and of the Netherlands Agency for Aerospace Programs (NIVR). The *ASCA* observation was performed as part of the joint ESA/Japan scientific program. This research has made wide use of data obtained through the High Energy Astrophysics Science Archive Research Center Online Service, provided by the NASA/Goddard Space Flight Center. This research has also made use of the SIMBAD database, operated at CDS, Strasbourg, France. ASM data were provided by the *RXTE* ASM teams at MIT and at the *RXTE* SOF and GOF at NASA's GSFC. We thank the anonymous referee for valuable comments. We also thank Massimo Cappi and Mauro Dadina for assistance in the *ASCA* data analysis, Stefano Bernabei for useful discussions on the optical spectra, and the staff astronomers of the Observatory of Bologna in Loiano for assistance during observations.

References

Anders, E., & Grevesse, N. 1989, Geochim. Cosmochim. Acta, 53, 197
Arnaud, K. A. 1996, XSPEC: the first ten years, in Proceedings of the V ADASS Symposium ed. G. H. Jacoby, & J. Barnes, ASP Conf. Ser., 101, 17
Barret, D., Olive, J. F., Boirin, L., et al. 2000, ApJ, 533, 329
Blackburn, J. K. 1995, in Astronomical Data Analysis Software and Systems IV, ed. R. A. Shaw, H. E. Payne, & J. J. E. Hayes, ASP Conf. Ser., 77, 367
Boella, G., Butler, R. C., Perola, G. C., et al. 1997a, A&AS, 122, 299
Boella, G., Chiappetti, L., Conti, G., et al. 1997b, A&AS, 122, 327
Bradt, H. V., Rothschild, R. E., & Swank, J. H. 1993, A&AS, 97, 355
Buccheri, R., Bennett, K., Bignami, G. F., et al. 1983, A&A, 128, 245
Chakrabarty, D., & Roche, P. 1997, ApJ, 489, 254

Chiappetti, L., & Dal Fiume, D. 1997, The XAS Data Analysis System, in Proceedings of the Fifth International Workshop on Data Analysis in Astronomy, ed. V. di Gesù, M. J. B. Duff, A. Heck, et al. (World Scientific Press), 101
Cooke, B. A., Ricketts, M. J., Maccacaro, T., et al. 1978, MNRAS, 182, 489
Corbet, R. H. D., & Peele, A. G. 2001, ApJ, in press [astro-ph/0107131]
Dal Fiume, D., Poulsen, J. M., Frontera, F., et al. 1990, Il Nuovo Cimento, 13 C, 481
Dal Fiume, D., Masetti, N., Bartolini, C., et al. 2000, ASCA and BeppoSAX observations of the peculiar X–ray source 4U 1700+24/HD 154791, in The Fifth Compton Symposium, ed. M. L. McConnell, & J. M. Ryan, AIP Conf. Proc., 510, 236 [astro-ph/0002348]
Dickey, J. M., & Lockman, F. J. 1990, ARA&A, 28, 215
Diodato, M. 1998, Laurea Degree Thesis, Dipartimento di Astronomia, Università di Bologna
Dumm, T., & Schild, H. 1998, NewA, 3, 137
Engvold, O., & Rygh, B. O. 1978, A&A, 70, 399
Fiore, F., Guainazzi, M., & Grandi, P. 1999, Technical Report 1.2, *BeppoSAX* scientific data center, available online at: ftp://www.sdc.asi.it/pub/sax/doc/software_docs/saxabc_v1.2.ps
Forman, W., Jones, C., Cominsky, L., et al. 1978, ApJS, 38, 357
Frank, J., King, A. R., & Raine, D. J. 1992, Accretion Power in Astrophysics (Cambridge Univ. Press, Cambridge)
Frontera, F., Dal Fiume, D., Robba, N. R., et al. 1987, ApJ, 320, L127
Frontera, F., Costa, E., Dal Fiume, D., et al. 1997, A&AS, 122, 357
Garcia, M. R., Baliunas, S. L., Doxsey, R., et al. 1983, ApJ, 267, 291
Gaudenzi, S., & Polcaro, V. F. 1999, A&A, 347, 473
Gierliński, M., Zdziarski A. A., Poutanen, J., et al. 1999, MNRAS, 309, 496
Gunn, J. E., & Stryker, L. L. 1983, ApJS, 52, 121
Haberl, F. 1995, A&A, 296, 685
Horne, K. 1986, PASP, 98, 609
Hünsch, M., Schmitt, J. H. M. M., Schröeder, K.-P., & Zickgraf, F.-J. 1998, A&A, 330, 225
Illarionov, A. F., & Sunyaev, R. A. 1975, A&A, 39, 185
Jacoby, G. H., Hunter, D. A., & Christian, C. A. 1984, ApJS, 56, 257
Jahoda, K., Swank, J. H., Stark, M. J., et al. 1996, in EUV, X–ray and Gamma-ray Instrumentation for Space Astronomy VII, ed. O. H. W. Siegmund, & M. A. Gummin, Proc. SPIE 2808, 59
Kazarovets, E. V., Samus, N. N., Durlevich, O. V., et al. 1999, IBVS 4659
Kubo, S., Murakami, T., Ishida, T., & Corbet, R. H. D. 1998, PASJ, 50, 417
Lang, K. R. 1992, Astrophysical Data: Planets and Stars (Springer-Verlag, New York)
Lammers, U. 1997, The SAX/LECS Data Analysis System User Manual, SAX/LEDA/0010
Leahy, D. A., Darbro, W., Elsner, R. F., et al. 1983, ApJ, 266, 160
Levine, A. M., Bradt, H. V., Cui, W., et al. 1996, ApJ, 469, L33
Liu, Q. Z., van Paradijs, J., van den Heuvel, E. P. J. 2001, A&A, 368, 1021
London, R. A., Taam, R. E., & Howard, W. M. 1986, ApJ, 306, 170
Manzo, G., Giarrusso, S., Santangelo, A., et al. 1997, A&AS, 122, 341
Makishima, K., Tashiro, M., Ebisawa, K., et al. 1996, PASJ, 48, 171
Merloni, A., Fabian, A. C., & Ross, R. R. 2000, MNRAS, 313, 193
Mewe, R., Groenschild, E. H. B. M., & van den Oord, G. H. J. 1985, A&AS, 62, 197
Mitsuda, K., Inoue, H., Koyama, K., et al. 1984, PASJ, 36, 741
Morgan, Jr., W. A., & Garcia, M. R. 2001, PASP, 113, 1386
Morrison, R., & McCammon, D. 1983, ApJ, 270, 119
Negueruela, I., Reig, P., Finger, M. H., & Roche, P. 2000, A&A, 356, 1003
Ohashi, T., Ebisawa, K., Fukazawa, Y., et al. 1996, PASJ, 48, 157
Owens, A., Oosterbroek, T., Parmar, A. N., et al. 1999, A&A, 348, 170
Parmar, A. N., Martin, D. D. E., Bavdaz, M., et al. 1997, A&AS, 122, 309
Perryman, M. A. C., Lindegren, L., Kovalevsky, J., et al. 1997, A&A, 323, L49; ESA, The Hipparcos and Tycho Catalogues, ESA SP-1200
Pfeffermann, E., & Briel, U. G. 1986, Proc. SPIE, 597, 208
Pfeffermann, E., Briel, U. G., Hippmann, H., et al. 1987, Proc. SPIE, 733, 519
Philip, A. G. D., & Hayes, D. S. 1983, ApJS, 53, 751
Predehl, P., & Schmitt, J. H. M. M. 1995, A&A, 293, 889
Raymond, J. C., & Smith, B. W. 1977, ApJS, 35, 419
Rothschild, R. E., Blanco, P. R., Gruber, D. E., et al. 1998, ApJ, 496, 538
Schaefer, B. E. 1986, PASP, 98, 556
Schlegel, D. J., Finkbeiner, D. P., & Davis, M. 1998, ApJ, 500, 525
Serlemitsos, P. J., Jalota, L., Soong, Y., et al. 1995, PASJ, 47, 105
Silva, D. R., & Cornell, M. E. 1992, ApJS, 81, 865
Smith, D. M., Heindl, W. A., Swank, J. H. 2001, ApJ, in press [astro-ph/0103304]
Sunyaev, R. A., & Titarchuk, L. 1980, A&A, 86, 121
Tanaka, Y., Inoue, H., & Holt, S. S. 1994, PASJ, 46, L37
Titarchuk, L. 1994, ApJ, 434, 570
Tomasella, L., Munari, U., Tomov, T., et al. 1997, IBVS 4537
Turner, M. J. L., Smith, A., & Zimmermann, H.-U. 1981, Space Sci. Rev., 30, 513
Turnshek, D. E., Turnshek, D. A., Craine, E. C., & Boeshaar, P. C. 1985, An atlas of digital spectra of cool stars (Western Research Company, Tucson)
Trümper, J. 1982, Adv. Space Res., 2(4), 241
van der Klis, M. 1995, Rapid aperiodic variability in X–ray binaries, in X–ray Binaries, ed. W. H. G. Lewin, J. van Paradijs, & E. P. J. van den Heuvel (Cambridge Univ. Press, Cambridge), 252
van der Klis, M. 2000, ARA&A, 38, 717
Voges, W., Aschenbach, B., Boller, T., et al. 1999, A&A, 349, 389
Wendker, H. J. 1995, A&AS, 109, 177
White, N. E., Kallman, T. R., & Swank, J. H. 1983, ApJ, 269, 264
Willson, L. A. 2000, ARA&A, 38, 573
Wu, K., Soria, R., Campbell-Wilson, D., et al. 2002, ApJ, 564, in press [astro-ph/0109222]
Yamashita, A., et al. 1997, IEEE Trans. Nucl. Sci., 44, 847